

INFLUENCE OF MODEL RESOLUTIONS IN HIGH-MOUNTAIN REGION: A VERIFICATION AGAINST OBSERVATIONS IN SELECTED CASE STUDIES

Raffaele Salerno

Research and Development, Epson Meteo Centre, Milan, Italy

1. INTRODUCTION

In the past five years many studies about numerical simulations in complex areas have been performed at Epson Meteo Centre (EMC). Particularly, hydrostatic (HY) and non-hydrostatic (NHY) computations have been made in many ideal and real cases (Salerno and Borroni, 2002), analyzing the differences among HY and NHY simulations at different resolutions in a complex topography and using a fully-compressible spectral model. Cascade runs were performed in a one-way nesting environment, choosing the characteristics of the finest grid domain in agreement to the examined phenomenon and, after that, establishing the sequence of coarser runs. The idealized barotropic and baroclinic instabilities showed that the solutions, in compressible mode runs, grow more slowly than their incompressible counterparts. The linear stability analysis evidenced that the growth rates, for both instabilities, decrease with compressibility. Simulations of barotropic and baroclinic instability in the NHY compressible mode were nearly identical to those using the HY one, but it appears that the relatively slow growth continues well into the nonlinear regime. Many real cases of mountain waves and penetrative convection were considered, evidencing that, for HY simulations, finer resolutions lead to stronger vertical motions associated with mountain waves and details of the mountain waves and high winds might have been poorly captured. With 10 and 5 km grid mesh sizes, the downstream tilt of the main wave in the HY case was much smaller than in the NHY one. Vertical structures of propagating plumes of vertical motion were stronger and fairly well organized in the NHY mode runs. Investigation of the behaviour of the semi-implicit, semi-lagrangian scheme in complex topography and many range of flows with idealized mountains (Salerno, 2003) were also analyzed in the recent years, using the same NHY spectral model.

Corresponding author address: Dr. Raffaele Salerno, Epson Meteo Center, via M.V. de Vizzi 93/95, 20092 Cinisello Balsamo (MI), Italy.
Email: raffaele.salerno@epson-meteo.org

It was shown that the treatment of spurious orographic resonances (Ritchie and Tanguay, 1996) might be unsuccessful at very-high resolution and a benefit can be obtained adding a smoothing filter which seemed to be effective due to the spectral nature of the model. Moreover, with a grid mesh size less than 3 km, the model needed a short time step, further away the greatest allowable one, to avoid an unsatisfactory representation of orographic waves. To take into account the mountain slope in a more accurate way, boundary conditions were improved. Many numerical simulations have been also made in the Himalayan and Indian areas by using a global and a regional model (Bollasina and Bertolani, 2004). This work shows some further results about the model resolution influence on weather predictions in a few high-mountain areas in the world considering some relevant case studies. Quite large grid meshes cannot resolve some characteristics of the circulations and, particularly in complex areas, the vertical wind velocities, which do not affect only dynamics, but the thermal and moisture distribution, which has an influence on the wind characteristics and the occurrence and strength of precipitations. High-resolution mesoscale simulations can get better results to describe the circulation patterns, the surface parameters and the precipitation amounts, to be compared to local and satellite observations. In the framework of an integrated modelling approach at regional and local scale, simulations were performed in the alpine area (Salerno, 2005). Results about precipitations fairly well agreed with observations, and the higher resolutions were crucial to improve the location and the values of the precipitations.

The simultaneous use of mesoscale models may give a further improvement in the description of weather dynamics and thermodynamics. Recent winter tests have been made comparing models prediction against observations on selected locations in the alpine region. Particularly, three models (WRF, EMC-MSM mesoscale model and MesoNH) have been used at "operational" resolutions ranging from 7 to 20 km. All models have shown quite good predictions detecting the precipitation episode with values fairly close to observations, even if the time location of the maxima resulted somewhat moved

(and slightly lower) respect to the observed ones, an aspect more evident with decreasing resolutions.

2. MODEL DESCRIPTION

Atmospheric models require heavy computer resources. The concurrent possibility to distribute the computation over a cluster of computer has been one of the basic ideas of the implementation of atmospheric modeling at EMC, with the load distribution handled by a cluster management system, which gives opportunities to make efficient use of systems. The research group of EMC has developed a parallel computation for weather forecasting both for global and regional domains, with a mesh grid size up to few hundredths of meters. Now, with the developing of our algorithms, a cluster of computer with different characteristics will be used to make high performance computations on atmospheric physics from global to local scale, both for operational weather forecasting and research. The whole system has been designed for high scalability and maximum flexibility, in order to satisfy the requirement of operational uses together with the research developments.

2.1 EMC-MSM

The EMC-MSM is a scalable and flexible model suitable for a wide range of atmospheric scales (Salerno and Borroni, 2002). An hydrostatic-pressure vertical coordinate is used for HY and NHY primitive equations. Conservation of total energy is assured by the continuity equation which is strictly retained. The time integration is semi-implicit and semi-Lagrangian. Lateral boundary relaxation is considered; it may be either explicit or implicit, time-splitting. A lateral boundary blending may be also considered and 4th order horizontal diffusion is applied. Since non-zero boundary conditions may cause serious difficulties with semi-implicit time schemes, perturbation method is applied for the resolution of the equation in the model, because zero lateral boundary condition can be satisfied and diffusion can be applied to perturbation only (Juang, 1992). The model uses a type of dynamical initialization which can be considered whenever there is a doubt about the balance state of the initial conditions or when a field such as vertical motion is not given in the initial analysis. But the initialization on the finer meshes is omitted when these are driven by coarser runs. Flux computation in the surface layer follows the Monin-Obukhov similarity profile (Arya, 1988) with a multi-layer soil model in which different classes of vegetation and soil types are considered. Vertical turbulent eddy diffusion of momentum, heat and vapour is computed in this study via a non-local

approach in the boundary layer where in the free atmosphere the formulation is based on scale parameters obtained from observation; another option available in the model is a Mellor-Yamada improved TKE scheme (Mellor and Yamada, 1982). Deep convection is treated with a relaxed Arakawa-Schubert scheme (Moorthi and Suarez, 1992, 1999); Kain-Fritsch (K-F) parameterization is also available (Kain and Fritsch, 1993). The microphysics treatment employs five prognostic species including water vapour, cloud water, cloud ice, snow and rain (Rutledge and Hobbs, 1983).

2.2 MesoNH

MesoNH is a mesoscale nonhydrostatic model developed by the Centre National de Recherches Meteorologiques (Meteo-France) and the Laboratoire d'Aerologie (CNRS). MesoNH is a numerical model able to simulate atmospheric motions at different scales, from the large meso-alpha scale down to the micro-scale. It is a grid point model and makes use of an Arakawa C-grid both for the horizontal and the vertical grid. The model makes use of the anelastic approximation in the resolution of the equations of motion. In this approximation the fluid is virtually incompressible or pseudo-incompressible. The time scheme is explicit; lateral boundary conditions are variable: cyclic, or rigid wall, or open or a combination of these different types of conditions can be chosen. MesoNH allows grid-nesting and two or more models can be run at the same time, with the possibility of a two-way interaction between the coarse and the fine mesh model at every time step. It is operationally nested in EMC-ESM, the European-scale version of the Epsom Meteo Centre model. Physiographic data (topography, soil-vegetation characteristics, etc.) can be given by the user, or data files are already present with a global domain and a resolution of 1 km for orography and surface cover type, and of 10 km for clay or sand fraction. For the microphysical scheme up to eight water species can be chosen (vapour water, cloud water, rain, ice, snow, graupel, hail and pristine ice), or a combination of these species (Pinty and Jabouille, 1998), and several cloud schemes can be used (usually the Kessler scheme is chosen for warm clouds). For deep convection K-F scheme is used.

Turbulence can be treated one-dimensionally where only the vertical turbulent fluxes are taken in account or three dimensionally where all the fluxes are computed (Cuxart et al., 2000). The turbulent mixing length can be calculated with different approaches selected by the user. To not cause major restrictions for the time step, because of the use of an explicit time scheme, for the vertical diffusion term a semi-implicit or fully implicit time scheme can be chosen. Also several options for the radiation scheme can be

chosen, but for a complete treatment of radiation the ECMWF radiation scheme is implemented.

2.3 WRF

The WRF model is a flexible, state-of-the-art, atmospheric model usable in a massively parallel computing environment (Wang et al., 2004). It offers numerous physics options, thus tapping into the experience of the broad modelling community. It is suitable for use in a broad spectrum of applications across scales ranging from meters to thousands of km. Such applications include research and operational numerical weather prediction, data assimilation and parameterized-physics research, downscaling climate simulations, driving air quality models, atmosphere-ocean coupling, and idealized simulations (e.g. boundary-layer eddies, convection, baroclinic waves). It is a fully-compressible, Euler NHY model with a run-time hydrostatic option available and it is conservative for scalar variables. Terrain-following hydrostatic-pressure, with vertical grid stretching permitted, is used as vertical coordinate (Laprise, 1992). Time integration is split-explicit using a 3rd order Runge-Kutta scheme with smaller time step for acoustic and gravity-wave modes. Second to sixth order advection options in horizontal and vertical are available. Sub-grid scale turbulence formulation in both coordinate and physical space. Divergence damping, external-mode filtering, vertically implicit acoustic step off-centring are considered. Explicit filter option are also available. Initial conditions may come from three-dimensional real-data. One-way, two-way, and moving nesting are provided. Microphysics uses bulk schemes ranging from simplified physics, suitable for mesoscale modelling, to sophisticated mixed-phase physics, suitable even for cloud-resolving modeling. The cumulus parameterizations are based on adjustment and mass-flux schemes for mesoscale modelling (Kain and Fritsch, 1993). Surface physics uses multi-layer land surface models ranging from a simple thermal model to full vegetation and soil moisture models (4 layers), including snow cover and sea ice. Turbulence scheme is based on turbulent kinetic energy prediction (Mellor and Yamada, 1982) or non-local K schemes. Atmospheric radiation physics adopt long-wave and short-wave schemes with multiple spectral bands; a simple shortwave scheme with cloud effects and surface fluxes is included. The domain is automatically decomposed for a multiprocessor

3. CASE STUDIES, ALPINE REGION

Many results have been obtained from particular real situations analyzed by the model. Some of them are presented, particularly three of them are winter

test in the alpine area: the first one is the 31st of December 2005, the second is the 26-27th of January 2006; the third one has been made by using the three models at a resolution of few km and compare the results in selected points in the Piedmont area, February 18-20, during the Olympic Winter Games. These cases are characterized by snow precipitation in the Northern Italy; the January case is particularly interesting due to the amplitude and the amount of snowfall, which produced the major snow event in the last 20 years.

3.1 December 31st, 2005

This case was characterized by a cold air mass coming from the Northern Europe with very low temperature in the night before, between -10°C and -15°C in the Po valley. Partially sunny during the day, with maximum temperature around 0°C at midday. In the evening, a frontal system from the Atlantic ocean hit the Northern and Western Italy, with freezing rain and snow which gave many problems in the main roads and highways. In Milan and in the evening, drizzle, snow grains and snow were recorded, while in Bergamo and Brescia snow were recorded after 7 p.m., but in the western part of Piedmont, for instance, no precipitation occurred (fig. 1).

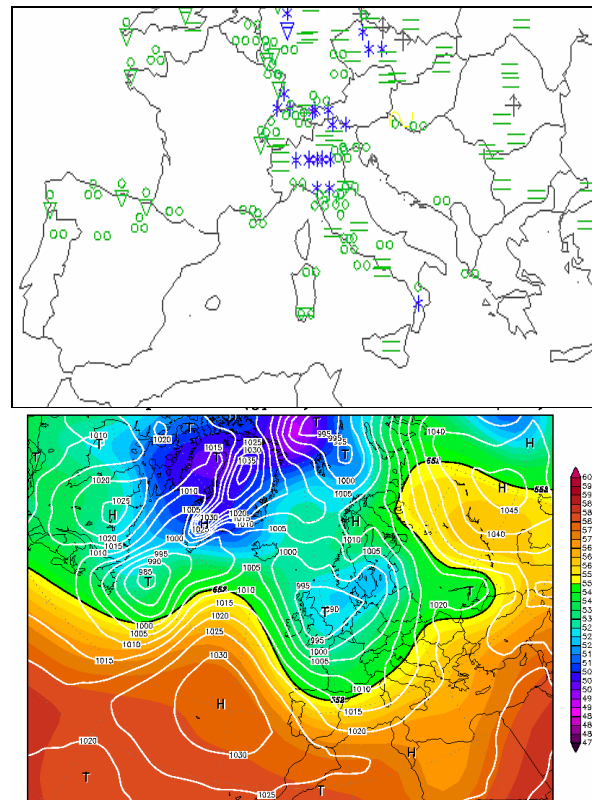


Fig. 1. Maps of weather at 00 UTC, January 1st, 2006. Snow, represented by a * in the upper image, is reported in the Po valley from Lombardia to Veneto. In the lower image SLP and 500 hPa from NCEP reanalysis are shown.

The figures from 2 to 4 show the three-hours sequence of precipitation type forecasted by MSM model at 18 and 21 UTC, Dec. 31st and 00-03 UTC, Jan. 1st, using a diagnostic module adapted from NCEP precipitation-type algorithm (Wandishin et al., 2005).

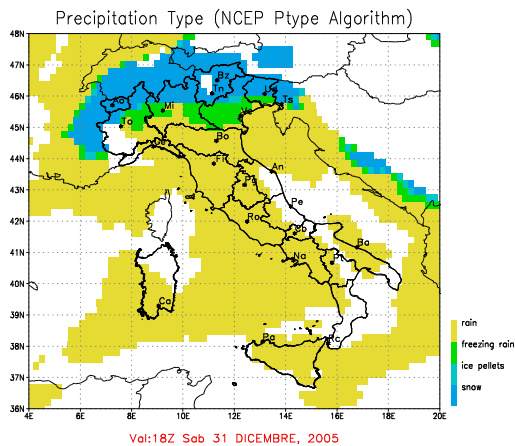


Fig. 2. Evolution of the precipitation type (December 31st, 2005, 18UTC), as forecasted by prediction system. Yellow areas are referred to rain, green areas are for freezing rain and blue and light-blue areas are for snow and ice pellets

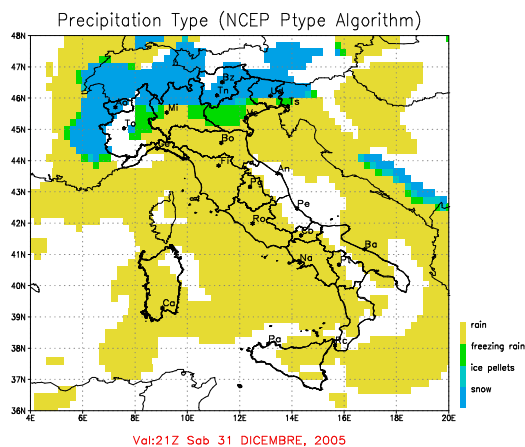


Fig. 3. Same as fig. 2 but at 21 UTC, December 31st, 2005

In this case, WRF and MSM ran at a resolution of 10 km while Meso-NH was at 20 km. Due to lower resolution, Meso-NH precipitation locations were slightly less defined. The type of precipitation is quite well reproduced compared to the observations recorded in that day. Particularly, the evolution of rain and freezing rain in some areas of the Po Valley has been correctly depicted. Fig. 5 represents the height level where the precipitation type becomes snow, considering an algorithm developed at Epson Meteo Centre. Here the map at 18 UTC of December 31 presents the height level at which the precipitation

is forecasted as snow and the 3-h accumulated precipitation.

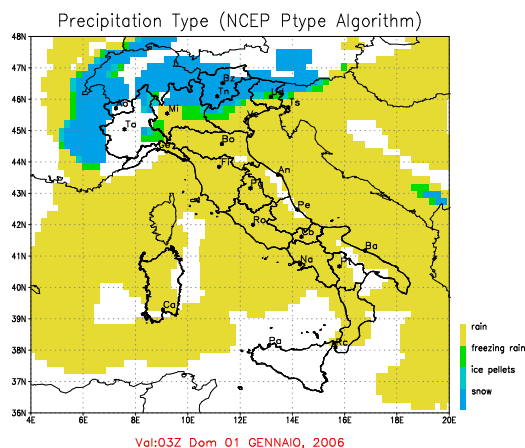
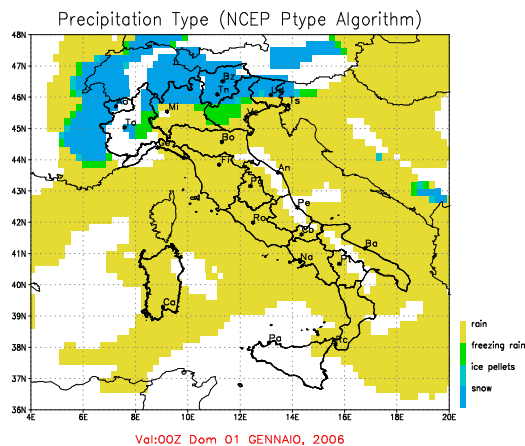


Fig. 4. Same as fig. 2 but at 00 and 03 UTC, January 1st, 2006

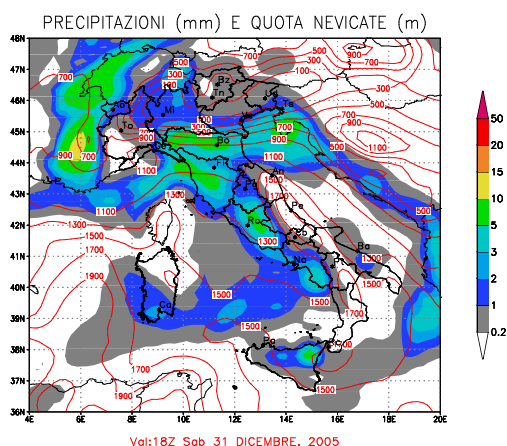


Fig. 5. Forecast of height of snowfall (a.s.l.) and 3-h accumulated precipitation at 18 UTC, Dec. 31st, 2005

3.2 January 26-27th, 2006

To have abundant snow in the south alpine region it is necessary a particular configuration of the atmospheric currents, which is characteristic for this type of event. Like in the previous cases, also this time, in the week before this snow event, the weather has been dominated from a definite area of high pressure on North-Eastern Europe, while cold continental air repeatedly flowed from east towards the alpine region and, particularly, the south alpine slope. The meteorological situation of winter stable weather is also usually marked from strong thermal inversions that carry to a further cooling of the low layers of the atmosphere. A low pressure on western Mediterranean Sea produced south and southeast wind toward the Alps, with humid air blocked by the mountains in the south alpine region (figure 6).

In the morning of the 26th of January, snow started to fall. Then, for about 48 hours, snow occurred in the Po valley and generally in Piedmont, Lombardia, Liguria, Emilia, Trentino. This has been the major snow event in the last 20 years for northern Italy, both for the extension and the amount of precipitation: 65 cm in Sondrio, 60 in Genoa, 55 in Como and Ovada, 50 in Novara, 45 in Lodi and Vercelli, 43 in Bergamo, 40 in Milan and Pavia, 35 in Alessandria, 30 in Biella and Brescia, 15 in Reggio Emilia.

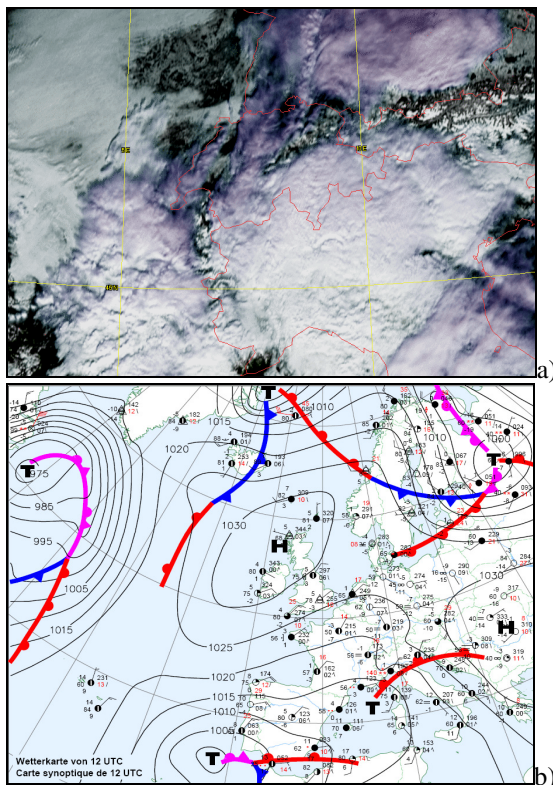


Fig. 6. Satellite image (a) and the synoptic chart (b) at 12 UTC of January 27th, 2006 (from MeteoSwiss).

The figures 7 and 8 show two forecast maps of precipitation type and height of snowfall at 12 UTC of January 27th, 2006. The area in light blue at the left represents the snow precipitation as computed by NCEP precipitation-type algorithm. The area extent is confirmed by the level of snowfall, represented by a red line on the right map. The total amounts of snowfall computed by all models were close to those observed by measurements, almost independently from the resolution ranging from 10 to 20 km.

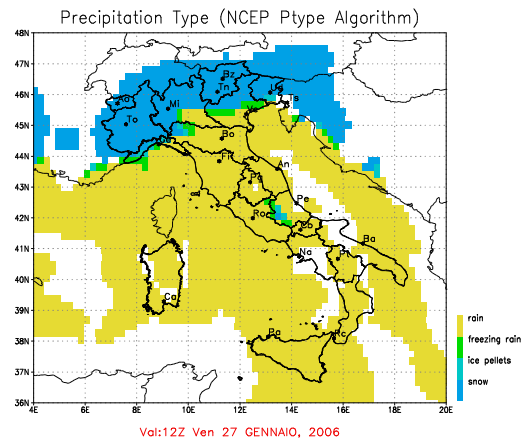


Fig. 7. Precipitation type at 12 UTC of January 27th, 20

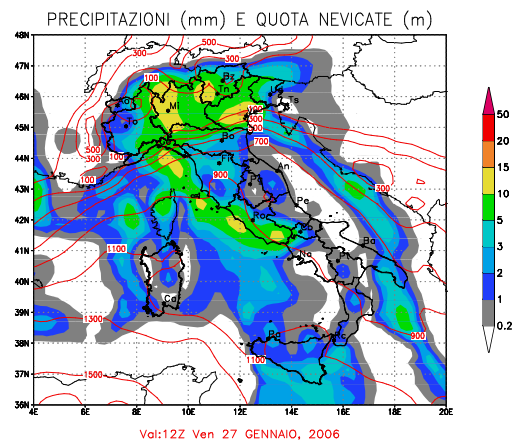


Fig. 8. Precipitation amount and height of snowfall at 12 UTC of January 27th, 2006

At the end of this snow episode, the western part of the Po Valley presented quite large areas of snow-covered land (fig. 9).

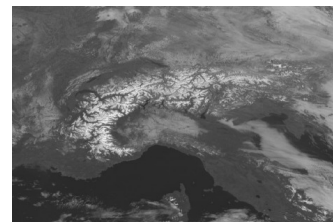


Fig. 9. Visible satellite image of January 31st, 2006.

3.3 February 18th -20th 2006

This situation was characterized by a couple of cold front crossing the alpine region: the first one February 18, and second one in the night of February 19 (fig. 10), when thunderstorms also occurred in the south alpine region, due to a temperature difference of about 30 °C between 850 and 500 hPa. This is an air mass cold enough to develop convective system also in winter.

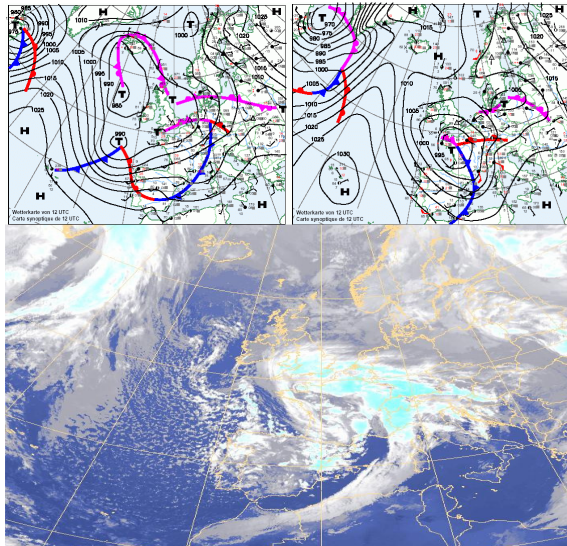


Fig.10. Synoptic charts of February 18-19 and the satellite image of 18 UTC, February 19 (from MeteoSwiss).

Precipitation locations and maxima were not well represented with resolution higher than 20 km. At 10 km, results were better but only at 5 km or less the results were quite good (fig. 11)

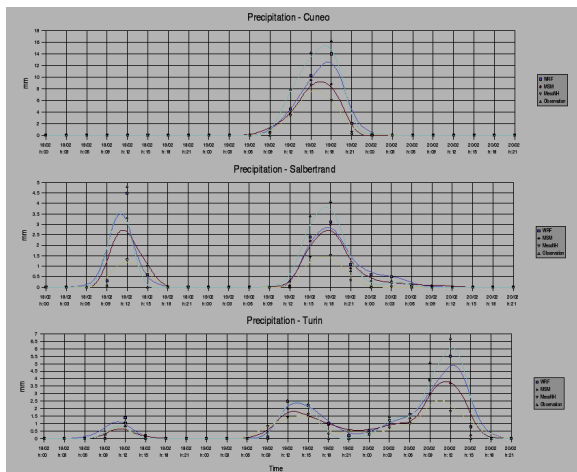


Fig. 11. The precipitation forecasted by the three models at 4 km of resolution in three places in the Piedmont area. Particularly, the first diagram is referred to a location near the Olympic mountain venue, while the last diagram is referred to Turin (observed data from Regione Piemonte).

4. HIMALAYAS CASE STUDIES

In the same framework, simulations have been made in the Indian region and, particularly in the Himalayas. This area is particularly studied at Epson Meteo Centre, since it is many year that exists a collaboration with the Italian National Research Council to study the climatology of the area and to simulate the monsoon circulation.

During summer a planetary-scale warm air mass is centred on south Asia with the maximum average layer temperature (>22 °C) over the southern Tibetan Plateau, resulting in strong temperature gradients in both the north-south and east-west directions. A warm temperature ridge exists also over the North American continent, and a deep temperature trough stretches from the west coast of North America to the central Pacific. A similar trough lies over the Atlantic Ocean. The upper tropospheric flow pattern during summer identifies clearly the thermal contrast between continents and oceans (Krishnamurti, 1971a, b). The boreal winter presents a very different structure. A much smaller section of the globe (northeast of Australia) is warmer than 26 °C. A warm temperature ridge lies over South America, and a slightly weaker ridge covers Australia. The regional and mesoscale considered areas have been depicted in the fig. 12.

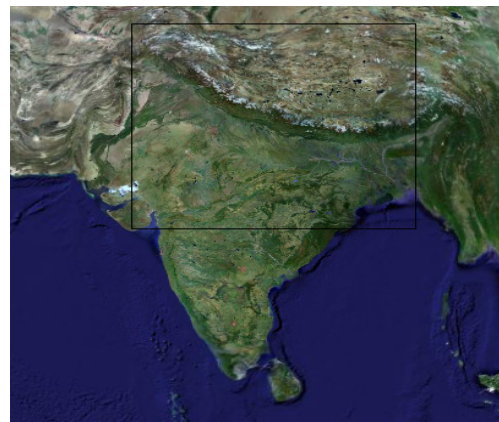


Fig.12. The regional and mesoscale area considered in the simulations

This time, the used models have been a GCM at 1° of resolution, regional and mesoscale models ranging from 50 to 10 km. Two case studies are briefly presented here.

4.1 June 10-16th, 2005

This is a situation occurred a couple of weeks before the monsoon onset (fig.13). Starting from June 10th, a 6 day to 1 day lagged forecast has been made to June 16th, using different regional and mesoscale models at various resolutions and comparing their results to 1°

GCM simulations, which also generally provided the boundary conditions to the regional and mesoscale simulations.

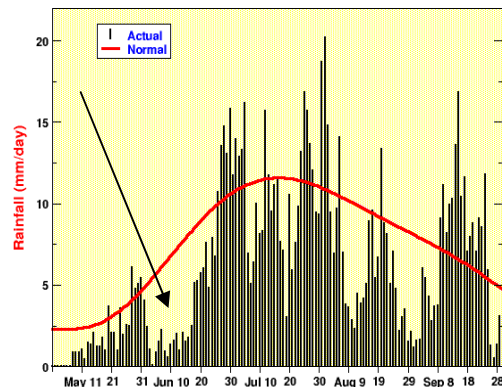


Fig. 13. 2005 and normal India monsoon rainfall. The arrow indicates the time period of case study (from All-India Summer Monsoon Rainfall, Indian Institute of Tropical Meteorology)

The comparison between the analysis data of June 16th 2005 (fig. 14) and the different lagged forecasts, have shown that this situation has been poorly represented at the global and regional scale, even quite close to the target day (figs 15-16). This may be partially caused by the uncertainty in the initial conditions and a poor representation of surface characteristics, with a consequent uncertainty in the surface processes which drive this particular situation.

More generally, the degree to which monsoon cycle is predictable depends upon the space scale and timescale for which predictability is being sought. The day-to-day changes in rainfall at any place are normally determined by the life cycle of synoptic scale disturbances (lows, depressions, monsoon trough, etc.) at or around the place of consideration. Thus, predictability of day-to-day weather at a point in the monsoon region should be in no way different from that of any other point on the globe and can be limited to a few days. However, the monsoon cycle could be driven by a statistical average of a variety of independent short-period fluctuations or large-scale evolving processes. In the first case there would be no greater predictability for the monsoons than would be expected for the extra-tropics. On the other hand, if the monsoon were controlled solely by large-scale evolving processes as slowly varying boundary conditions at the Earth's surface or very low frequency changes that determine, for instance, the inter-annual behaviour of the seasonal mean monsoon circulation and rainfall, and the inter-annual variability of the short period fluctuations is controlled by such large-scale low-frequency forcing, one would expect that the limits of monsoon prediction would be given by the limits of

predictability of the planetary-scale forcing functions. However, if there were large-scale and low-frequency instabilities of the monsoon which might, for example, determine the intra-seasonal active and break periods of the monsoon, then one may expect hybrid limitations to predictability existing somewhere short-period fluctuations and large-scale low frequency forcing. In the pre-monsoon situation, and before the onset, this hybrid limitation might occur also in the short-range predictions if the local effects, the reproduction of energy cascade and the interaction between large scale circulation and local scale dynamics and thermodynamics, considering the terrain characteristics (soils, canopies, topography) are not adequately represented.

At a resolution of 15 km or less there is an abrupt change in the model simulations at the mesoscale; with these resolutions, the situation is almost correctly represented (figs. 15 and 17), and even the 5-day simulation reproduces fairly well the geopotential field in the upper troposphere.

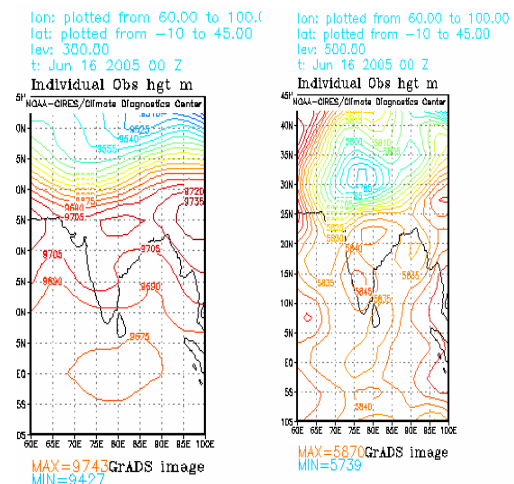


Fig. 14 The 300 and 500 hPa analysis of June 16th, 2005 from CDC

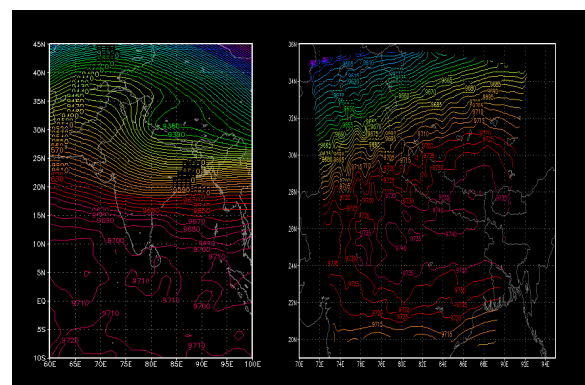


Fig. 15. The 300 hPa 5-day forecast for 00 UTC of June 16. Regional simulation is on the left, mesoscale high-resolution simulation on the right.

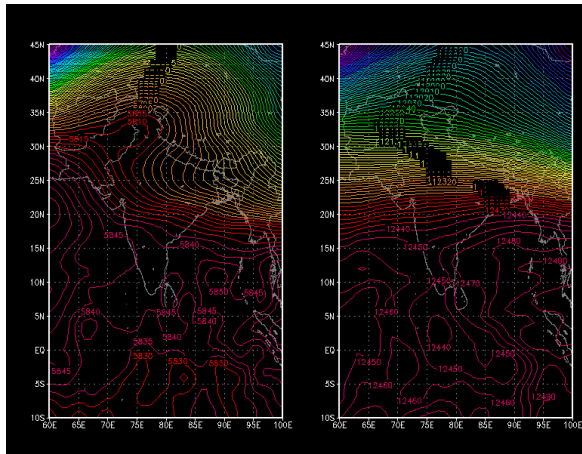


Fig. 16. 500 and 200 hPa 2-day forecast at regional scale for 00 UTC of June 16.

shows less uncertainties in the initial and boundary conditions and a minor importance of the surface details and resolutions in the forecast, showing also how large-scale low-frequency fluctuations drive this kind of situation.

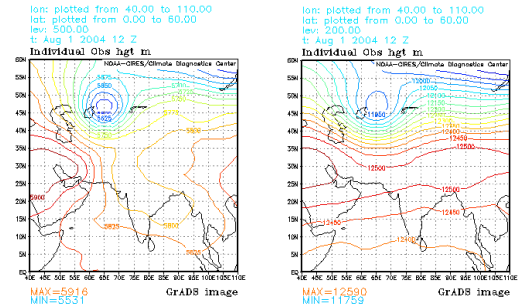


Fig. 18. 500 and 200 hPa analysis at 12 UTC, August 1st, 2004.

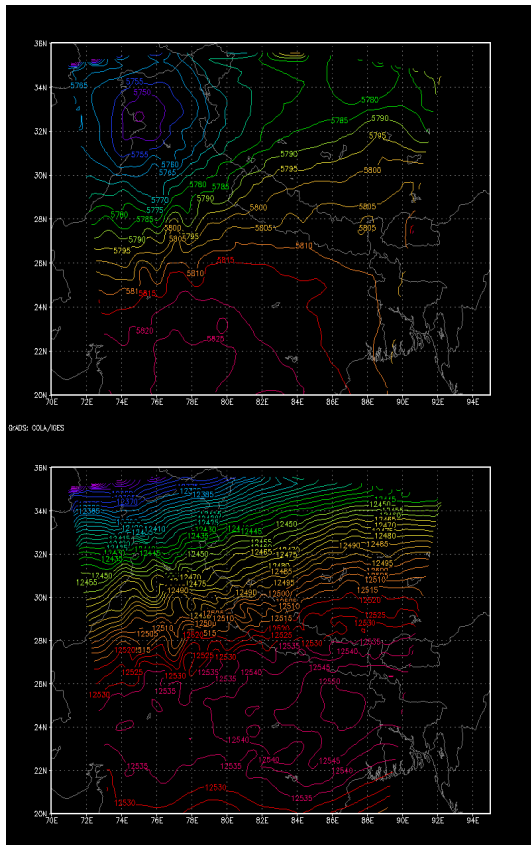


Fig. 17. 500 (above) and 200 hPa 2-day high resolution mesoscale simulation for 00 UTC of June 16.

4.2 August 1st, 2004

The time location of this case is in the active phase of the monsoon season. Considering the discussion of the previous case, this situation has been correctly represented even by the GCM (figs. 18 and 19) and

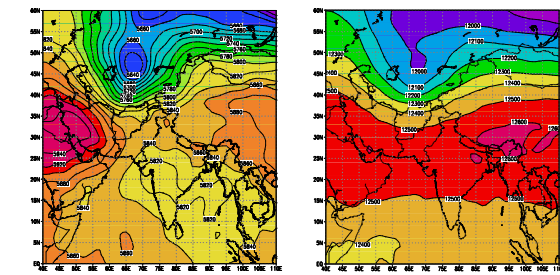


Fig. 19. 500 and 200 hPa 2-day forecast at 12 UTC, August 1st, 2004

5.CONCLUSION

GCMs contain representations of the atmosphere, oceans, ice, land surface and vegetation, but they are incomplete if resolution is poor compared to terrain characteristics. Regional models may give a deeper insight in the dynamics and the physics in high complex terrain. Low resolutions may somewhat fail in describing the correct dynamics. Comparing the time series of the observations with model outputs, high resolution is fundamental to incorporate as much as possible the local effects, the reproduction of energy cascade and the interaction between large scale circulation and local scale dynamics and thermodynamics, considering the terrain characteristics.

The simultaneous use of mesoscale models may give a further improvement in the description of weather dynamics and thermodynamics. Recent winter tests have been made comparing models prediction against observations on selected locations in the alpine region. Particularly, three models (WRF, CEM mesoscale model and MesoNH) have been used

at different resolutions. All models have generally shown quite good predictions detecting the precipitation episode with values close to observations, even if the time location of the maxima resulted somewhat moved and slightly lower respect to the observed ones, an aspect more evident with lower resolutions. In the Himalayas, a case in the weeks before the 2005 monsoon onset has shown a very strong dependence on resolutions of the model results, suggesting a possible existence of threshold value, a situation never found in the alpine region. This is probably due to short-period fluctuations which can be adequately represented only when surface characteristics are well represented in such an area where north-south and east-west gradients are very strong, but further investigations are required.

References:

- Arya, S. P., 1988: *Introduction to Micrometeorology*. International Geophysics Series, vol. **42**, Academic Press inc.
- Bollasina, M. and L. Bertolani, 2004: Winter Snow over the Himalayas: Observations and Simulations during CEOP EOP-3. *Proc. 2nd Asia Pacific Ass. of Hydrol. And Water Res. Conf.*, 5-8 July, Singapore, Vol. **2**, 492-501.
- Cuxart, J., Bougeault, Ph. and Redelsperger, J.L., 2000: A Turbulence Scheme Allowing for Mesoscale and Large-Eddy Simulations. *Q. J. R. Meteorol. Soc.*, **126**, 1-30.
- Juang, H.-M. H., 1992: A Spectral Fully Compressible Nonhydrostatic Mesoscale Model in Hydrostatic Sigma Coordinates: Formulation and Preliminary Results. *Meteor. Atmos. Phys.*, **50**, 75-88.
- Kain, J. S., and J. M. Fritsch, 1993: *Convective parameterization for mesoscale models: The Kain-Fritsch scheme. The representation of cumulus convection in numerical models*. K. A. Emanuel and D. A. Raymond, Eds., Amer. Met. Soc., 246 pp.
- Krishnamurti, T. N., Observational study of the tropical upper tropospheric motion field during the northern hemisphere summer, *J. Appl. Meteorol.*, **10**, 1066-1096, 1971a.
- Krishnamurti, T. N., Tropical east-west circulation during the northern summer, *J. Atmos. Sci.*, **28**, 1342-1347, 1971b.
- Laprise R., 1992: The Euler Equations of Motion with Hydrostatic Pressure as an Independent variable. *Mon. Wea. Rev.*, **120**, 197-207.
- Mellor, G. L., and T. Yamada, 1982: Development of a Turbulence Closure Model for Geophysical Fluid Problems. *Rev. Geophys. Space Phys.*, **20**, 851-875.
- Moorthi, S., and M.J. Suarez, 1992: Relaxed Arakawa-Schubert: A parameterization of moist convection for general circulation models. *Mon. Wea. Rev.*, **120**, 978-1002.
- Moorthi, S., and M.J. Suarez, 1999: *Documentation of version 2 of Relaxed Arakawa-Schubert cumulus parameterization with moist downdrafts*. NOAA Technical report NWS/NCEP 99-01. 44 pp.
- Pinty, J.-P. and P. Jabouille, 1998. A Mixed-Phase Cloud Parameterization for Use in Mesoscale Nonhydrostatic Model: Simulations of a Squall Line and of Orographic Precipitations. *Proc. Conf. of Cloud Physics*, Everett, WA, USA, Amer. Meteor. soc., Aug. 1999, 217 - 220.
- Rutledge, S. A. and P. V. Hobbs, 1983 : The mesoscale and microscale structure and organization of clouds and precipitation in midlatitude cyclones. Part VIII: A model for the "seeder-feeder" process in warm-frontal rainbands. *J. Atmos. Sci.*, **40**, 1185-1206.
- Ritchie, H. and M. Tanguay, 1996: A Comparison of Spatially-Averaged Eulerian and Semi-Lagrangian Treatment of Mountains. *Mon. Wea. Rev.*, **124**, 167-181.
- Salerno, R. and A. Borroni, 2002: Hydrostatic vs. Nonhydrostatic Simulations in a Complex Orography Environment. *Proc. of 10th Conf. on Mountain Meteorology*, 17-21 June, Park City, Utah, 299-302.
- Salerno, R., 2003: Influence of Nonhydrostatic Effects and Time-Integration Schemes on Numerical Simulations in a Complex Orography Environment. *Publ. of MeteoSwiss*, no. 66, 230-233.
- Salerno, R., 2005: Model Inter-Comparison for research and Operational Use: a Case-Study in the Alpine Region. *Croatian Meteorol. Publ.*, vol. **40**, 423-426.
- Wang, W., D. Barker, C. Bruyère, J. Dudhia, D. Gill, and J. Michalakes, 2004. *WRF Version 2 Modelling System User's Guide*.